

## Supporting Information for

# Orientation Dependent Physical Transport Behavior and Micro-mechanical Response of ZnO Nanocomposites Induced by SWCNT and Graphene: Importance of Intrinsic Anisotropy and Interfaces

*Xin Liang\*, Yuqing Yang, Feihu Dai, and Changan Wang*

School of Materials Science and Engineering, Changzhou University, Changzhou,  
Jiangsu 213164, China

\*Corresponding author (X. Liang): liangxin@cczu.edu.cn

Table SI. Mass densities, relative mass densities (calculated based on ZnO), and spark plasma sintering (SPS) conditions of samples studied in this work.

Samples		SPS conditions	Density (g/cm <sup>3</sup> )	Relative density
ZnO	Disc	800 °C 70 MPa	5.53	99%
	Cylinder	5 min	5.59	99%
1 wt% SWCNT/ZnO	Disc	800 °C 70 MPa	5.38	96%
	Cylinder	5 min	5.20	93%
2 wt% SWCNT/ZnO	Disc	900 °C 70 MPa	5.23	93%
	Cylinder	5 min	5.20	93%
1 wt% G/ZnO	Disc	800 °C 70 MPa	5.17	92%
	Cylinder	5 min	5.13	92%
2 wt% G/ZnO	Disc	900 °C 70 MPa	5.40	96%
	Cylinder	5 min	5.26	94%

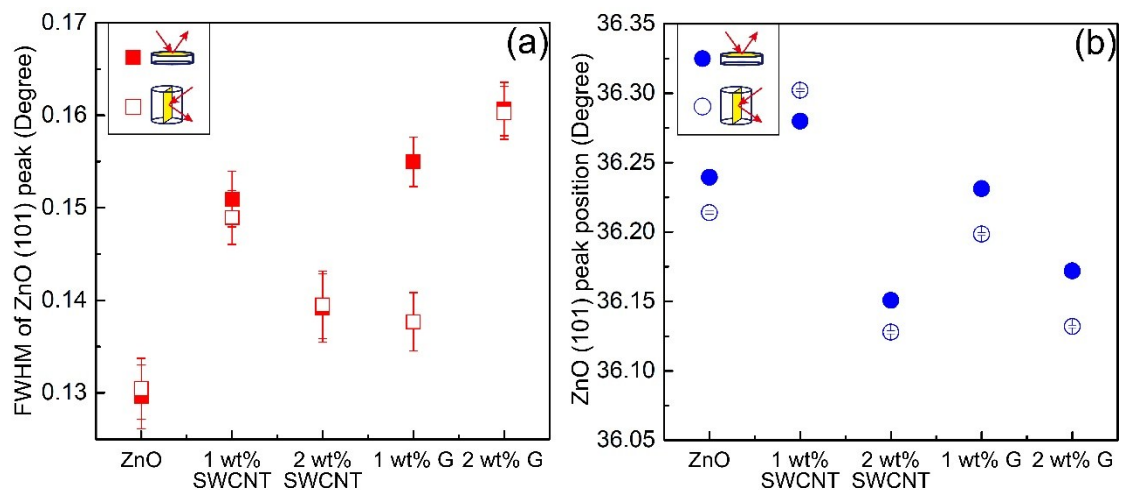


Figure S1. (a) FWHM (full width at half maximum) and (b) XRD peak position for ZnO (101) in all samples for two measurement orientations, obtained from the profile analysis of XRD patterns.

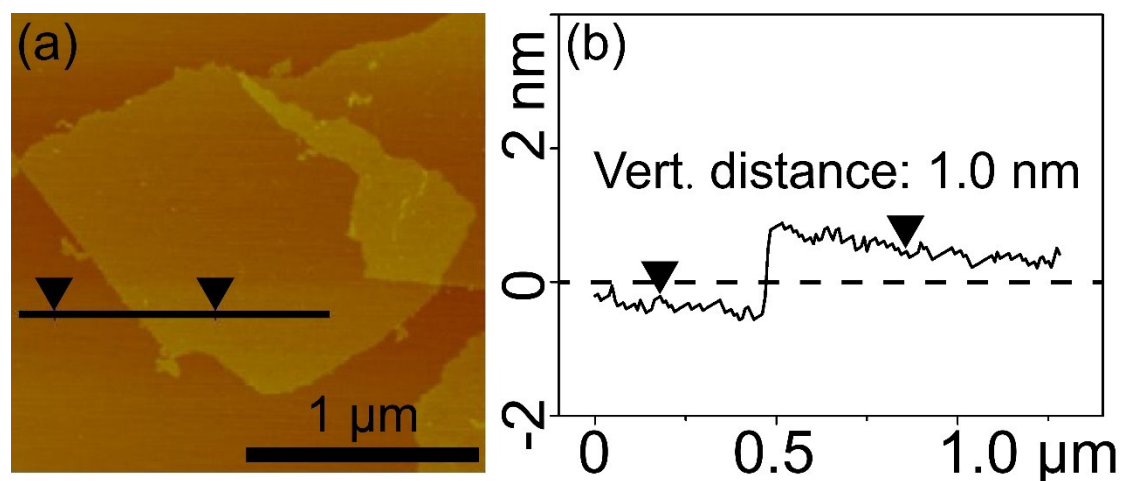


Figure S2. Atomic force microscopy (AFM) image of graphene used in this work and the corresponding topology profile as a function of lateral distance showing the thickness of graphene flake about 1.0 nm.

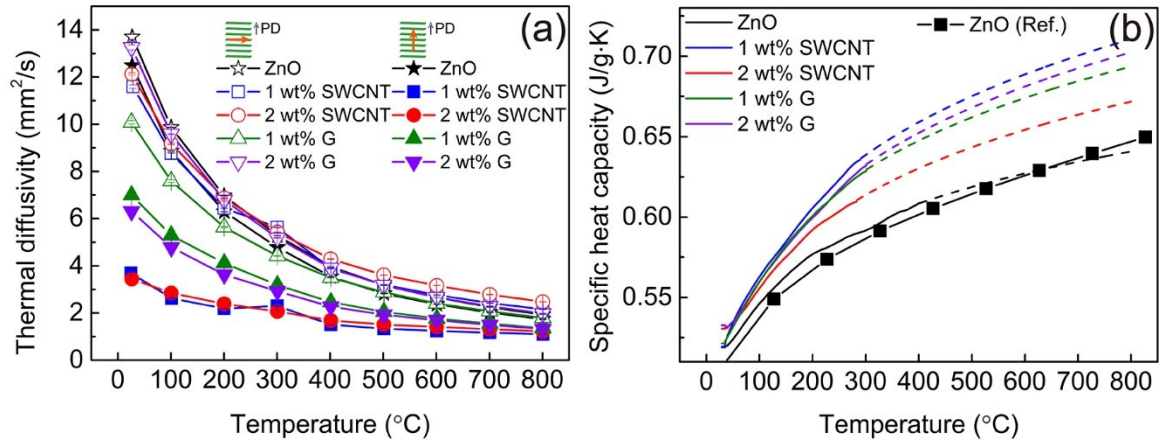


Figure S3. Temperature dependent thermal diffusivity (a) and specific heat capacity (b) measured along the directions that are parallel and perpendicular to the sample pressing direction (PD), respectively. The dashed lines of DSC curves in (b) are extrapolated data for elevated temperatures due to the fluctuated measured raw data above 300  $^{\circ}\text{C}$ . Our DSC-measured specific heat capacities of pure ZnO (black solid line) agree well with the reference data (filled square symbols) <sup>1</sup>.

Table SII. The Interfacial thermal (Kapitza) resistances for four types of ZnO/carbon thermal interfaces,  $ZnO/SWCNT_{Axial}$ ,  $ZnO/SWCNT_{Radial}$ ,  $ZnO/G_{In-plane}$ , and  $ZnO/G_{Cross-plane}$ , derived from the thermal conductivity measured for in-plane and cross-sectional transport directions.

Samples	ZnO/carbon thermal interfaces	Kapitza resistance ( $m^2K/W$ )
1 wt% SWCNT/ZnO	$ZnO/SWCNT_{Axial}$	$R_{ZnO/SWCNT}^{Axial} = 1.4 \times 10^{-6}$
	$ZnO/SWCNT_{Radial}$	$R_{ZnO/SWCNT}^{Radial} = 5.6 \times 10^{-6}$
2 wt% SWCNT/ZnO	$ZnO/SWCNT_{Axial}$	$R_{ZnO/SWCNT}^{Axial} = 2.7 \times 10^{-6}$
	$ZnO/SWCNT_{Radial}$	$R_{ZnO/SWCNT}^{Radial} = 3.4 \times 10^{-6}$
1 wt% G/ZnO	$ZnO/G_{In-plane}$	$R_{ZnO/G}^{In-plane} = 42.5 \times 10^{-6}$
	$ZnO/G_{Cross-plane}$	$R_{ZnO/G}^{Cross-plane} = 6.8 \times 10^{-6}$
2 wt% G/ZnO	$ZnO/G_{In-plane}$	$R_{ZnO/G}^{In-plane} = 38.0 \times 10^{-6}$
	$ZnO/G_{Cross-plane}$	$R_{ZnO/G}^{Cross-plane} = 3.6 \times 10^{-6}$

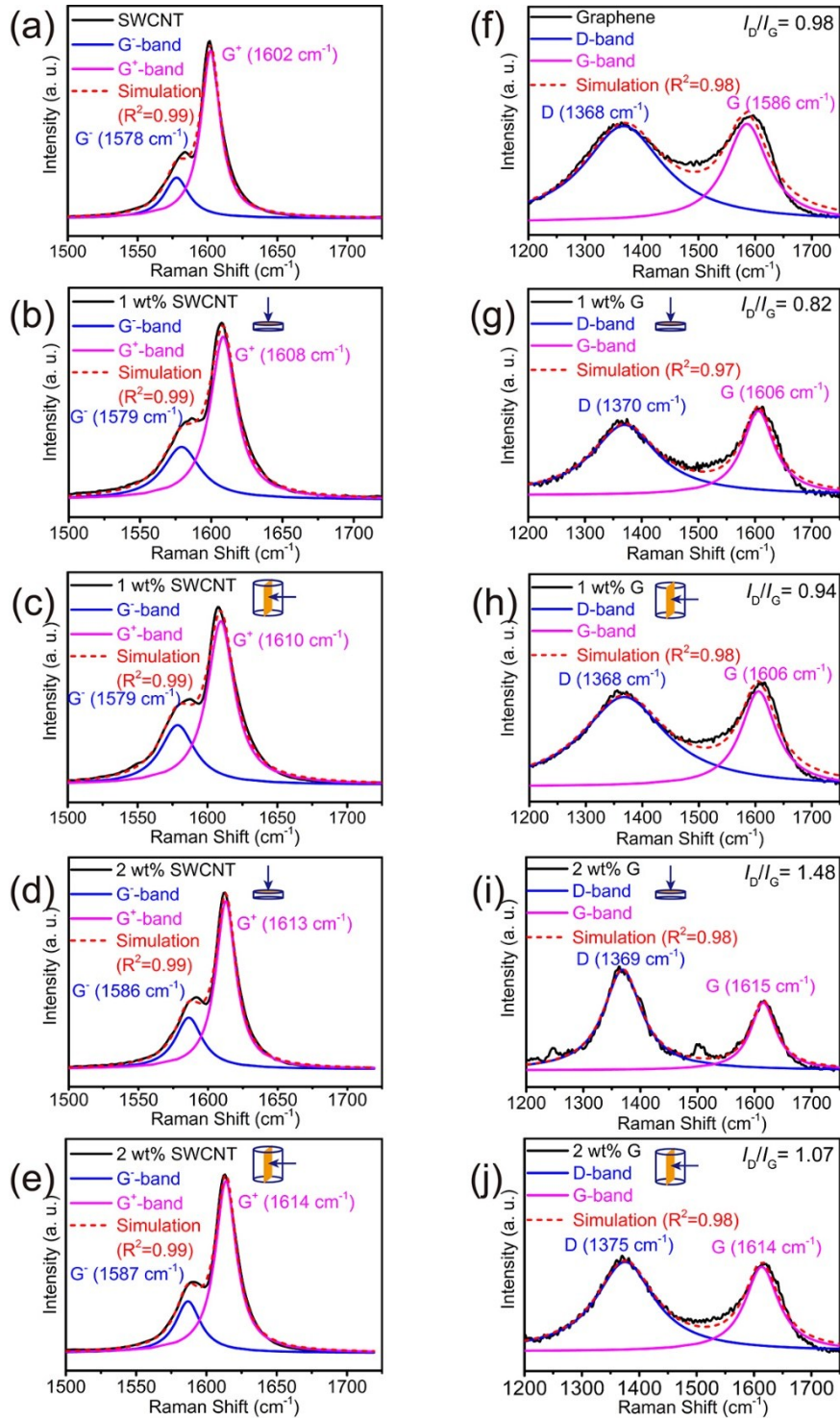


Figure S4. Analysis of Raman  $G^+$  and  $G^-$  peaks for SWCNTs, and  $G$  and  $D$  bands for graphene in SWCNT/ZnO (b-e) and G/ZnO (g-j) nanocomposites. For each nanocomposite sample, the analysis was made for the Raman spectra collected from the top-view and cross-sectional planes of samples, respectively. The analysis for pristine SWCNT (a) and graphene (f) are also made for reference.

## References

1. I. Barin, *Thermochemical data of pure substances*, VCH, Weinheim, 1989.